Reorganisation of diffusion microstructure in the precuneus is associated with preserved cognitive function in Parkinson's disease

Atsuko Nagano-Saito (Atsuko.nagano@gmail.com)
McGill University
Jean-Christophe Houde
Université de Sherbrooke
Christophe Bedetti
Centre Hospitalier de l'Université de Montréal
Maxime Descoteaux
Université de Sherbrooke
Marco Leyton
McGill University
Chawki Benkelfat
McGill University
Oury Monchi
University of Calgary

Research Article

Keywords: medial prefrontal cortex, anterior cingulate cortex, posterior cingulate cortex, precuneus, PD-nonMCI, PD-MCI

DOI: https://doi.org/10.21203/rs.3.rs-147275/v1

Abstract

Functional neuroimaging studies of patients with Parkinson's disease (PD) have repeatedly identified over-activations in midline structures (medial prefrontal cortex, anterior cingulate cortex, posterior cingulate cortex, and precuneus), especially in those without comorbid dementia. Here, we investigated whether the different cognitive profiles in PD were linked to measures of diffusion microstructure in medial regions of the brain. Using magnetic resonance based diffusion weighted imaging (DWI) in healthy volunteers (HV) and PD patients with and without mild cognitive impairment (PD-nonMCI and PD-MCI), applying diffusion tensor imaging (DTI) and high angular resolution diffusion imaging (HARDI) techniques, we observed: 1) increased fractional anisotropy (FA) in the precuneus and the anterior cingulate in the PD-nonMCI participants compared with the HV; 2) an association between precuneus FA and executive and memory function, respectively, in PD and HV; 3) a negative correlation between age and midline structure FA in PD but not HV; and 4) a differential association between cognitive scores and apparent fiber density (AFD) of the posterior cingulate-precuneus bundle in HV vs. PD. Together, these findings suggest that white matter reorganization of the posterior medial microstructures might serve a compensatory role for damaged basal ganglia function in PD-nonMCI.

Introduction

Parkinson's disease is a progressive neurodegenerative disorder caused by the loss of dopamine neurons [1]. Motor symptoms emerge after more than 50 to 80% of nigrostriatal dopaminergic neurons have lost their function [2–4] with a prodromal phase occurring at least a few years beforehand [3,5]. The main symptoms are considered to be the motor dysfunction, but, in some patients, cognitive deficits are present even at early stages of the disease [6]. The motor and cognitive impairments are associated with dopamine deficiency in the striatum within parallel cortico-basal ganglia-thalamocortical circuits [7–10], and positron emission tomography (PET) studies of PD patients have identified impaired striatal dopaminergic function associated with both motor [11–14] and cognitive problems [11,13,15,16]. These observations are paralleled by functional magnetic resonance imaging (MRI) studies, which have shown reduced motor circuit activity associated with motor dysfunction [17–19] and reduced cognitive circuit activity associated with cognitive impairments [20–23].

In contrast to these neurological deficits, PD patients have also been repeatedly reported to exhibit over-activations in the medial prefrontal cortex [18,19] and lateral prefrontal cortex [17,24] during the performance of motor tasks, and over-activation in the precuneus during cognitive tasks [21,25]. These increases appear to become greater as the disease progresses, and larger task-induced activations in the medial prefrontal cortex and precuneus have been observed at 2-year follow-up compared to the first scan in non-demented PD patients both with and without mild cognitive impairment [26]. Moreover, resting state fMRI measures have identified increased hub function in the anterior part of the precuneus and the posterior cingulate cortex in PD patients without cognitive impairment (PD-nonMCI), but not in PD patients with mild cognitive impairment (PD-MCI), and hub function in these posterior medial structures was positively

correlated with cognitive function in all PD patients [27]. In part, these alterations might be related to dopamine perturbations, and a positron emission tomography study identified evidence of upregulated anterior cingulate dopaminergic projections associated with motor dysfunction [14]. Together, these observations may indicate that an upregulation of midline structures play an important role in supporting motor and cognitive functions in PD patients, likely by compensating for the dysfunction of cortico-basal ganglia thalamocortical circuits, possibly beginning during the prodromal phase.

The hypothesized upregulation of midline neurocircuitry might be associated with microstructure changes in structural connectivity. This can be tested with local microstructural measurement of water diffusion through diffusion-weighted MR imaging (DWI), with diffusion tensor imaging (DTI) [28–31] and high angular resolution diffusion imaging (HARDI) techniques (Descoteaux and Deriche, 2007; Jensen et al., 2005; Ozarslan et al., 2006; Tournier et al., 2007; Tuch, 2004). A recent meta-analysis of DTI studies of PD patients vs. age-matched healthy volunteers [37] yielded evidence of significant differences in DTI measures in the substantia nigra and corpus callosum, subcortically, and in the cingulate and temporal cortices, cortically, indicating degeneration in PD. Several studies have shown that various parts of the corpus callosum have higher microstructural organization, indicated by higher FA or lower diffusivity, in patients with PD compared to HV [38–40]. Cognitive function of PD patients was associated with widespread degeneration of white matter, especially, in the frontal and temporal, and cingulate areas [41–44]. DTI requires an assumption of Gaussian diffusion of water, which may not occur in biological tissues. To overcome this limitation, newer techniques have been developed to analyse DWI [35,36,45]. Using one of them, diffusion kurtosis imaging, it was reported that FA in the anterior cingulate, but not in the posterior cingulate, was significantly lower in PD patients, compared with HV [46]. This may indicate that the microstructure of the posterior cingulate is relatively preserved in PD patients, and that it could compensate PD's dysfunction of the cortico-basal ganglia-thalamocortical circuits, especially for cognitive function in early stage. High angular resolution diffusion imaging (HARDI) technique is another one. It further enables us to create fiber orientation distribution function (fODF) models [32–36], which offer accurate tractography and apparent fiber density (AFD) for each streamline [47,48]. Here, we aimed to see if changes in microstructure measures of the medial regions are associated with cognitive function in PD patients, using DTI and HARDI techniques. With this method, we predicted associations between a reorganization of the posterior part of the midline structure and cognitive function in PD.

Results

Demography

The participants were 38 PD patients at stages I and II of Hoehn and Yahr (mean age +/- SD, 62,0 +/- 5.0 years; range, 53 to 69; 24 male and 14 female), who were divided into 2 groups: those with MCI (n = 18) and those who were cognitively intact (non-MCI, n = 20), and 16 healthy volunteers (HV; mean age +/- SD, 61.8 +/- 5.5 years; range, 53 to 72; 7 male and 9 female) without cognitive impairment. A comprehensive neuropsychological evaluation, targeting 5 cognitive domains: attention and working memory, executive

functions, language, memory, and visuoperceptual abilities (Supplementary Table 1), was administered before the scanning session.

As shown in Supplementary Table 2, expected group differences were evident between HV vs PD (all), for Montreal Cognitive Assessment (MoCA) scores ($p = 0.012$), Beck depression inventory (BDI) scores ($p = 0.0018$), Brixton Z-scores, as an indicator of executive function ($p = 0.010$), and RAVLT Z-scores, as an indicator of memory function ($p = 0.027$). PD-nonMCI vs HV had elevated BDI scores ($p = 0.012$) and trended toward lower Brixton Z-scores ($p = 0.076$). Between PD-nonMCI and PD-MCI, significant differences were observed in age ($p = 0.021$) and RAVLT Z-scores ($p = 0.038$), and a marginally significant difference was observed in Brixton Z-scores ($p = 0.083$). The two PD groups did not differ on Unified Parkinson's Disease Rating Scale (UPDRS), motor examination.

Group comparison of fractional anisotropy (FA) and mean diffusivity (MD)

After pre-processing the diffusion weighted imaging (DWI) data, diffusion tensor image (DTI) analyses were applied to create fractional anisotropy (FA), and mean diffusivity (MD) matrices for each participant, and a region of interested analysis was done, using four sets of regions of interest (ROIs) (Fig. 1-a). These four sets of ROIs were selected based on our previous studies (Nagano-Saito et al., 2004, 2016, and 2019). Compared to the HV, the PD-nonMCI had elevated FA values in the precuneus ($p = 0.041$) and anterior cingulate gyrus (ACG) ($p = 0.017$). Compared to the PD-nonMCI group, PD-MCI participants had higher MD values in the precuneus ($p = 0.026$) (Fig. 2), and this difference remained when age was added as a covariate ($p = 0.05$).

Correlation analysis of FA with age, Brixton, and RAVLT Z-scores

Results are summarized in Tables 1, for HV and PD, separately. RAVLT Z-scores and age tended to positively correlate with the precuneus FA in HV ($r = 0.691$, $p = 0.003$, and $r = 0.440$, $p = 0.088$, respectively), whereas in PD participants, precuneus FA was positively and negatively correlated, respectively, with Brixton Z-scores and age ($r = 0.350$, $p = 0.031$, and $r = -0.390$, $p = 0.015$, respectively) (Tables 1, Fig. 3). When age was covaried out, the significant correlation survived between the Precuneus FA and RAVLT Z-score ($r = 0.62$, $p = 0.015$), in HV, and marginal correlation was observed between Precuneus FA and Brixton Z-scores in PD ($r = 0.277$, $p = 0.097$). The FA in all the midline structures were strongly negatively correlated with age in PD, but not in HV. Correlation ratios were significantly different between the HV and PD, for Precuneus-FA and age, Precuneus-FA and Brixton Z-scores, and Precuneus-FA and RAVLT Z-scores, respectively ($Z = 2.724$, $p = 0.0032$; $Z = 2.0719$, $p = 0.0191$, and $Z = 2.9033$, $p = 0.0018$, respectively) (Fig. 3).

Tractography

High angular resolution diffusion imaging (HARDI) was applied on the DWI data to create fiber orientation distribution function (fODF) models. From the models, we extracted five bundles, for each hemisphere; 1) including the anterior part of the precuneus, but not the posterior part of the precuneus, and the posterior cingulate (PCG-Precuneus), 2) including the posterior cingulate and the parahippocampal area (PCG-PHG), 3) including the precuneus and the parahippocamal area, but not the posterior cingulate (Precuneus-PHG), 4) including the precuneus and the paracentral area, the primary motor area, but not the posterior cingulate (Precuneus-Cortex), and 5) including the precuneus but not extending to the posterior cingulate, parahippocampal area, or paracentral area (Precuneus-Local). Additionally, 6) one cross-hemisphere bundle was extracted including the both sides of the precuneus via the corpus callosum (Precuneus-Cross). The averaged track density images in MNI standard-space, of the six maps are shown in blue-green for HV (Fig. 1-c, the location of the corresponding maps not being different for the other two groups, PD-nonMCI and PD-MCI). The PCG-PHG bundle (Fig. 1-c, top middle) was located more laterally than the PCG-Precuneus bundle (Fig. 1-c, top left) in the PCG portion, then ran into the PHG. Among the six bundles, PCG-Precuneus (top left), Precuneus-Cortex (Fig. 1-c, bottom left), and Precuneus-Local (Fig. 1-c, bottom middle) were denser than other three bundles (Fig. 4).

Group comparison of apparent fiber density (AFD) index

For each streamline, with fODF models, apparent fiber density (AFD) index was estimated using the MRtrix3 package [49]. Significant differences in AFD index were observed in the Precuneus-Cortex between HV and PD-nonMCI ($p = 0.0036$), and in PCG-PHG between HV and PD-nonMCI ($p = 0.047$) and between PD-nonMCI and PD-MCI ($p = 0.048$) (Fig. 4). The latter effect was weakened but otherwise similar when age was added as a covariate ($p = 0.098$).

Correlation analysis of AFD index, with age, Brixton, and RAVLT Z-scores

Results are summarized in Tables 1, for HV and PD, separately. In HV PCG-Precuneus, AFD index tended to positively correlate with age and RAVLT Z-scores ($r = 0.511$, $p = 0.043$, and $r = 0.432$, $r = 0.094$, respectively), and negatively correlate with Brixton Z-scores ($r = -0.449$, $p = 0.081$) (Table 1, and Fig. 5). In PD, AFD index in the same bundle were negatively correlated with RAVLT Z-scores ($r = -0.382$, $p = 0.018$), and this survived when age was added as a covariate ($r = -0.413$, $p = 0.011$) (Table 1, and Fig. 5). PD participants also exhibited negative correlations between AFD index in the Precuneus-Cross bundle and age ($r = -0.610$, $p < 0.001$) (Table 1, and Fig. 5). Correlation ratios were significantly different between the HV and PD, for PCG-Precuneus AFD index and age, and AFD index and RAVLT Z-scores ($Z = 2.275$, $p = 0.0115$, and $Z = 2.662$, $p = 0.0039$)), and for Precuneus-Cross AFD index and age ($Z = 2.903$, $p = 0.0018$). A marginal difference was observed between the HV and PD, for PCG-Precuneus AFD index and Brixton Z-scores ($Z = 1.393$, $p = 0.0818$).

Discussion

We interrogated a DWI dataset with DTI and HARDI techniques to test whether brain midline microstructure is associated with cognitive function in patients with PD. Our primary findings were, 1) increased FA in the precuneus and the anterior cingulate in the PD-nonMCI participants compared with HV, which was not observed in PD-MCI participants; 2) precuneus FA was associated with executive and memory function, respectively, in PD and HV; 3) midline structure FA was negatively correlated with age in PD, but not in HV; and 4) the AFD index of the posterior cingulate-precuneus bundles were differentially associated with cognitive scores in HV and PD.

To our knowledge, this is the first study showing increased FA in the midline structure (the cingulate gyrus) in PD-nonMCI patients, compared with HV. FA in DTI is the most robust metric for quantifying diffusion anisotropy [50,51]. Increased FA can reflect diminished axonal branching, increased axonal myelination [52], or axonal sprouting [53]. Functional neuroimaging studies have repeatedly shown increased activity in the midline structure in PD patients vs. controls. This over-activation has been reported in the medial prefrontal cortex [18,19] and precuneus [21,25] while performing motor and cognitive tasks. During cognitive tasks, reduced deactivation in the default mode network, including the anterior and posterior midline structure, has also been reported in PD patients [54–56]. This might include a dopamine component, and upregulation of dopaminergic projections in the anterior cingulate cortex are associated with PD motor dysfunction [14]. These features appear to change as the disease progresses, and a longitudinal study showed greater activation in the midline structure at the second time compared to the first time in PD with and without mild cognitive impairment (Nagano-Saito et al, 2016). Increased hub function in PD-nonMCI has also been observed in the posterior part of the midline structure [27]. Our present findings regarding the FA change, together with these previous studies, possibly reflects increased axonal packing or sprouting, rather than diminished axonal branching, in the midline structure of the PD-nonMCI patients.

Mean diffusivity (MD) represents the average diffusivity of the component and provides a generalized measure of diffusivity in the area, and is nonspecific with respect to the directionality of the diffusion process [57]. Increased MD has been reported in disease-related neurodegeneration [58,59], and is thought to reflect decreases in membrane density due to cell degeneration [60]. We observed increased precuneus MD but not decreased precuneus FA, in the PD-MCI, compared with PD-nonMCI (Fig. 4). In addition to dysfunction of the cognitive cortico-basal ganglia-thalamocortical circuit in PD patients [7–10], the cognitive deficits in PD patients are also originating from cortical Lewy Body/alpha-synuclein deposits that can occur in posterior regions of the brain [61]. We speculate that the possible increased axonal packing or sprouting speculated in PD-nonMCI is not preserved in PD-MCI because of the increased neurodegeneration occurring in the latter group.

Correlation analyses with the cognitive Z-scores yielded statistically significant associations only in the precuneus FA. In the HV group, RAVLT Z-scores was positively correlated with the FA, whereas in the PD group, Brixton Z-scores was positively correlated with FA (Tables 1, Fig. 3). This would indicate that the precuneus cognitive contribution has a bigger effect on memory in HV, and a bigger effect on executive function in PD. Supporting this interpretation, there is evidence that the precuneus is involved in memory

retrieval in HV [62]. This observation may indicate that the possible increased axonal packing or sprouting in midline regions in PD-nonMCI patients compensates for executive dysfunction resulting from the impairment of the cortico-basal ganglia-thalamocortical circuits in PD, as we have previously proposed based on resting state fMRI data [27].

Although FA and MD are robust metrics for quantifying diffusion anisotropy, they do not provide information about streamlines passing the ROIs. They are voxel averages. This is why the AFD [47,48] were calculated. AFD indicates relative white matter fibre density per unit volume of tissue and we computed total AFD of associated streamlines belonging to specific bundles, normalized by the mean streamline length [47,63,64]. Based on the results of group comparisons of FA and MD, we were most interested in the bundle of the PCG-Precuneus and Precuneus-PHG, which included the precuneus ROI in Fig. 1-a. While significant differences in AFD index were not observed in PD-nonMCI compared with HV in those bundles (Fig. 4), significant correlation of the Precuneus-FA was only observed with the PCG-Precuneus AFD index ($r = 0.64$, $p = 0.0070$, in HV; $r = 0.39$, $p = 0.015$ in PD, respectively), and not with other bundles AFD index (Supplementary Table 3).

There were significant differences of correlation patterns between the HV and PD, for PCG-Precuneus AFD index and age, and AFD index and RAVLT Z-scores (Fig. 5). In the HV, significant positive correlation with age, marginally negative correlation with the Brixton Z-scores, and marginal positive correlation with the RAVLT Z-scores with AFD index were observed, whereas in PD patients, negative correlation with the RAVLT Z-scores occurred. We propose that the PCG-Precuneus bundle, which are important for HV to support memory, is used for supporting executive function in PD, but that reorganization of other bundles also could support cognitive function, resulting in the positive correlation between Precuneus FA and Brixton scores in PD.

We have previously shown that the dopamine in the postmedial cortex including the precuneus has an important role for network regulation [65]. The location of the PCG-Precuneus bundle seems to follow the D2/3 dopamine receptors distribution in the midline of our previous positron emission tomography study [65]. Therefore, we compared the location of the six bundles of our present study to the D2/3 receptor distribution from our previous study, and the PCG-Precuneus bundle overlapped significantly with the D2/D3 distribution (Supplementary Fig. 1). Although all of the neurotransmitters associated with this possible compensation are unknown, we propose that dopamine in the postmedial cortex might at least partially contribute to this.

In HV, marginally positive correlations between the Precuneus FA and age, and significantly positive correlation between PCG-Precuneus AFD index and age, were observed (Table 1). To our knowledge, significant positive correlation between the posterior part of the midline microstructure and age in HV has not been reported. FA decreases in most part of the brain with age; however, in some specific regions, FA increases with age [66]. The microstructure in the cingulum shows relative preservation with age [67]. Thus, microstructure measurements for specific regions and their corresponding bundles may show positive correlations with age. More studies are required to investigate this finding further. Contrary to the HV

group, we observed a strong negative correlation between the FA in the midline structure and age in PD patients (Table 1). With AFD, the Precuneus-Cross bundle, connecting the left and right hemisphere via corpus callosum, showed a significantly negative correlation with age in PD patients (Table 1, Fig. 5). Moreover, the positive correlation observed between the PCG-Precuneus bundle and age in HV disappeared in PD patients, and when the correlation rate in HV and in PD was compared, a significant difference was observed ($p = 0.015$). We hypothesize that the midline structure upregulates its hub function for cognition in PD patients [27], as long as the compensation potential is preserved.

This compensation process would start during the prodromal phase, which occurs at least a few years beforehand [3,5], accompanied by axonal packing or sprouting. A previous study indicated that early-stage PD patients (Hoehn and Yahr 1) showed increased white matter density of the corpus callosum, compared with HV and compared with more advanced stage PD patients (Hoehn and Yahr 2) [38], in accordance with our present results. At the time of disease onset, the compensation could occur in a limited fashion, resulting in the negative correlation between precuneus FA and age.

The proposed compensation mechanism in the prodromal phase, possibly associated with motor dysfunction, would be supported by reorganization in the posterior part of the brain prevalently, through the midline structure. This may explain why FA in the precuneus, but not the AFD index of PCG-Precuneus bundle, reached statistical significance when comparing HV and PD-nonMCI. Finally, although the present observations support and extend previous findings, DWI acquisition b-values were relatively low and the sample sizes were modest, underscoring the need for replication.

Using DWI data with DTI and HARDI techniques in HV and PD patients, we observed increased FA in the precuneus in PD-nonMCI but not in PD-MCI compared with HV, and change of association between AFD of the posterior midline structure and cognition. In accordance with our previous studies (Nagano-Saito et al., 2016, 2019), we propose that the posterior medial structure is overrecruited, plausibly reorganizing parts of the memory-related diffusion microstructures into executive function-related ones, in PD-nonMCI patients, to possibly compensate for damaged basal ganglia function.

Methods

Participants

The participants were 38 PD patients at stages I and II of Hoehn and Yahr (mean age +/- SD, 62,0 +/- 5.0 years; range, 53 to 69; 24 male and 14 female) diagnosed by a movement disorder neurologist and who met the UK brain bank criteria for idiopathic PD [68], and 16 healthy volunteers (HV; mean age +/- SD, 61.8 +/- 5.5 years; range, 53 to 72; 7 male and 9 female) without cognitive impairment. All participants underwent a cognitive assessment and MRI session. The majority of participants (PD 35; HV 16) were reported in a previous study [69], and 31 PD patients were involved in a functional MRI study [23]. All provided informed consent, and the protocol was approved by the Research Ethics Committee of the Regroupement Neuroimagerie Québec. Based on a comprehensive neuropsychological assessment, the

PD patients were divided into 2 groups: those with MCI (n = 18) and those who were cognitively intact (non-MCI, n = 20). MCI inclusion criteria were as follows: (1) objective evidence of cognitive decline: performance > 1.5 SD below standardized mean on 2 or more subtests within a cognitive domain ; (2) subjective complaint of cognitive decline from the patient or accompanying person; (3) absence of significant decline in daily living activities; and (4) absence of dementia as diagnosed by the evaluating neuropsychologist; consistent with newly proposed guidelines (Level II, comprehensive assessment) for diagnosis of MCI in PD patients by the Movement Disorder Society task force [70]. The HV group also underwent the same neuropsychological assessment and none of them met the criteria for MCI.

Neuropsychological assessment

A screening test, the Montreal Cognitive Assessment [71], and a comprehensive neuropsychological evaluation was administered before the scanning session. The comprehensive neuropsychological evaluation targeted 5 cognitive domains: attention and working memory, executive functions, language, memory, and visuo-spatial abilities (Supplementary Table 1).

MRI scanning

Participants were scanned at the Institut Universitaire de Gériatrie de Montréal's 3T Siemens TIM MRI scanner. Sessions began with a high-resolution, T1-weighted, 3D volume acquisition for anatomic localization (1 mm^3, voxel size), followed by a diffusion-weighted image (DWI) acquisition using a 2-D spin-echo EPI sequence, consisting of 64 diffusion-encoding gradients with a b of 700 s/mm^2, 75 slices (matrix size, 128 x 128 pixels, voxel size, 2 x 2 x 2 mm^3).

MRI data preprocessing

The DWI data were processed following the same methods as our previous study (Hanganu et al, 2018). Briefly, after denoising, up-sampling, and brain-masking, diffusion tensor image (DTI) analyses were applied to create fractional anisotropy (FA), and mean diffusivity (MD) matrices for each participant, and high angular resolution diffusion imaging (HARDI) was applied to create fiber orientation distribution function (fODF) models. From fODF models of each participant, tractography of five million streamlines of the whole brain was generated using a step size of 0.5mm.

DTI matrices

The T1-weignted image (T1WI) was non-linearly co-registered into the DWI b0 image, and the co-registered T1WI was non-linearly transformed into MNI-152 space. Using the transformation parameters, the FA and MD images were resampled into MNI-152 space. A region of interest (ROI) analysis was done. According to our hypothesis, based on our previous studies (Nagano-Saito et al., 2004, 2016, and 2019), four sets of ROIs, one for each hemisphere were located in the precuneus, isthmus, posterior cingulate, and anterior cingulate white matters. The diameter of the ROI was 7mm. These ROIs are shown in Fig. 1-a for the left hemisphere. Mean values of the FA and MD were values calculated for each ROI of each participant. Further, the mean values were averaged for corresponding left and right ROIs for each participant.

HARDI tractography and apparent fiber density

The T1WI image co-registered into the DWI b0 image was segmented into subcortical, cortical, and white matter parcellations, using the Freesurfer package [72], and thirty-four gyral based regions were parcellated per hemisphere using the Desikan–Killiany atlas [73]. The parcellations of the precuneus were further separated into anterior and posterior subregions. To get the subregions, first, the MNI-152 template was segmented, using the Freesurfer package. Then, the segmented precuneus on the MNI-152 template was manually divided into anterior and posterior subregions using the precuneal sulcus as the boundary. These subregions were used to extract specific streamlines, which included the precuneus ROI above. These subregions were then transformed into the individual space, using FSL package, applying the parameter of transformation from the MNI-152 space into the individual space. Using white matter query language (WMQL; Wassermann et al., 2016), we extracted five bundles, for each hemisphere; 1) including the anterior part of the precuneus, but not the posterior part of the precuneus, and the posterior cingulate (PCG-Precuneus), 2) including the posterior cingulate and the parahippocampal area (PCG-PHG), 3) including the precuneus and the parahippocamal area, but not the posterior cingulate (Precuneus-PHG), 4) including the precuneus and the paracentral area, the primary motor area, but not the posterior cingulate (Precuneus-Cortex), and 5) including the precuneus but not extending to the posterior cingulate, parahippocampal area, or paracentral area (Precuneus-Local). Additionally, 6) one cross-hemisphere bundle was extracted including the both sides of the precuneus via the corpus callosum (Precuneus-Cross). The extracted methods for 1) ~ 4) are summarized in Fig. 1-b.

The PCG-Precuneus bundle was set based on our previous study indicating increased hub function in the anterior part of the precuneus and the posterior part of the cingulate gyrus [27]. The PCG-PHG and Precuneus-PHG bundles were set based of our previous studies indicating that hippocampal compensation is used to maintain cognitive abilities in PD patients [26,75]. We also considered the cingulum bundles in the human beings, reported previously [76].

For each streamline, with fODF models, apparent fiber density (AFD) index was estimated using the MRtrix3 package [49]. All tract-specific fibre orientation distribution integrals within the fibre voxels belonging to a specific bundle were added and divided by the mean pathway length resulting in the AFD index [47,63,64]. The AFD index were averaged for corresponding left and right bundles for each of the five bundles. We did not include Precuneus-striatum bundle, as the number of them were very limited.

Group comparisons, and correlation analysis with diffusion microstructures vs age and cognitive scores

With the FA and MD, as well as with the AFD index of each bundle, group comparisons were performed, between the HV and non-MCI PD patients, and between the non-MCI and MCI PD patients. Based on our previous study (Nagano-Saito et al, 2014, 2016 and 2019), correlations were calculated between the diffusion microstructure markers, FA and AFD, and age, Z-scores of cognitive tasks of Brixton Switching test (executive function) [77] and RAVLT (delay-recall list: memory function) [78] in HV and in PD patients collapsing both MCI and nonMCI groups, separately. These three factors (age, Brixton Z-score, and RAVLT

Z-score) did not show any significant correlations each other ($p > 0.1$) in HV and in PD, respectively. For the group comparisons and correlation analyses, the significance threshold was set at $p = 0.05$. Because of our strong hypothesis, based on our previous studies (Nagano-Saito et al., 2014, 2016, and 2019), correction for multiple comparison was not applied.

Declarations

Acknowledgments

This study received funding from the Tourmaline Chair in Parkinson's disease and the Canadian Research Chair in non-motor symptoms of Parkinson's disease to OM. We thank the Institutional Research Neuroinformatics Chair to Prof M Descoteaux.

Authors' contributions

All authors contributed to the study conception and design. Material preparation, data collection and analysis were performed by Atsuko Nagano-Saito Jean-Christophe Houde, Christophe Bedetti, and Maxime Descoteaux. The first draft of the manuscript was written by Atsuko Nagano-Saito and all authors commented on previous versions of the manuscript. All authors read and approved the final manuscript.

Competing interests

There are no conflicts interest/competing interests.

Data Availability

The data associated with this article are available on request from the authors.

Ethics declarations for human experiments

All provided informed consent, and the protocol was approved by the Research Ethics Committee of the Regroupement Neuroimagerie Québec, in accordance with the 1964 Helsinki Declaration.

Consent to participate

Informed consent for participating the study was obtained beforehand from each participant.

Consent for publication

Informed consent for publication was obtained beforehand from each participant.

References

1. Lang, A. E. & Lozano, A. M. Parkinson's disease. First of two parts. *The New England journal of medicine***339**, 1044–1053 (1998).
2. Bernheimer, H., Birkmayer, W., Hornykiewicz, O., Jellinger, K. & Seitelberger, F. Brain dopamine and the syndromes of Parkinson and Huntington Clinical, morphological and neurochemical correlations. *Journal of the Neurological Sciences***20**, 415–455 (1973).
3. Fearnley, J. M. & Lees, A. J. Ageing and parkinson's disease: Substantia nigra regional selectivity. *Brain***114**, 2283–2301 (1991).
4. Braak, H. *et al.* Staging of brain pathology related to sporadic Parkinson's disease. *Neurobiology of Aging***24**, 197–211 (2003).
5. Nurmi, E. *et al.* Rate of progression in Parkinson's disease: A 6-[18F]fluoro-L-dopa PET study. *Movement Disorders***16**, 608–615 (2001).
6. Foltynie, T., Brayne, C. E. G., Robbins, T. W. & Barker, R. A. The cognitive ability of an incident cohort of Parkinson's patients in the UK. The CamPaIGN study. *Brain***127**, 550–560 (2004).
7. DeLong, M. R. *et al.* Role of basal ganglia in limb movements. *Human neurobiology***2**, 235–244 (1984).
8. Alexander, G. E., Delong, M. R. & Strick, P. L. Parallel organization of funtionally segregated circuits linking basal ganglia and cortex. *Annual Review of Neuroscience***9**, 357–381 (1986).
9. Divac, I., Rosvold, H. En. & Szwarcbart, M. K. Behavioral effects of selective ablation of the caudate nucleus. *Journal of Comparative and Physiological Psychology***63**, 184–190 (1967).
10. Owen, A. M. *et al.* Fronto-striatal cognitive deficits at different stages of Parkinson's disease. *Brain***115 (Pt 6**, 1727–1751 (1992).
11. Holthoff-Detto, V. A. *et al.* Functional effects of striatal dysfunction in Parkinson disease. *Archives of Neurology***54**, 145–150 (1997).
12. Leenders, K. L. *et al.* The Nigrostriatal Dopaminergic System Assessed in Vivo by Positron Emission Tomography in Healthy Volunteer Subjects and Patients With Parkinson's Disease. *Archives of Neurology***47**, 1290–1298 (1990).
13. Rinne, J. O. *et al.* Cognitive impairment and the brain dopaminergic system in Parkinson disease: [18F]fluorodopa positron emission tomographic study. *Archives of Neurology***57**, 470–475 (2000).
14. Nagano-Saito, A. *et al.* Cognitive- and motor-related regions in Parkinson's disease: FDOPA and FDG PET studies. *NeuroImage***22**, 553–561 (2004).
15. Ito, K. *et al.* Striatal and extrastriatal dysfunction in Parkinson's disease with dementia: a 6-[18F]fluoro-L-dopa PET study. *Brain : a journal of neurology***125**, 1358–1365 (2002).
16. Sawamoto, N. *et al.* Cognitive deficits and striato-frontal dopamine release in Parkinson's disease. *Brain : a journal of neurology***131**, 1294–1302 (2008).
17. Haslinger, B. *et al.* Event-related functional magnetic resonance imaging in Parkinson's disease before and after levodopa. *Brain***124**, 558–570 (2001).

18. Sabatini, U. *et al.* Cortical motor reorganization in akinetic patients with Parkinson's disease. *Brain***123**, 394–403 (2000).
19. Rowe, J. *et al.* Attention to action in Parkinson's disease. *Brain***125**, 276–289 (2002).
20. Lewis, S. J. G., Dove, A., Robbins, T. W., Barker, R. A. & Owen, A. M. Cognitive impairments in early Parkinson's disease are accompanied by reductions in activity in frontostriatal neural circuitry. *The Journal of neuroscience : the official journal of the Society for Neuroscience***23**, 6351–6356 (2003).
21. Monchi, O. Neural Bases of Set-Shifting Deficits in Parkinson's Disease. *Journal of Neuroscience***24**, 702–710 (2004).
22. Ekman, U. *et al.* Functional brain activity and presynaptic dopamine uptake in patients with Parkinson's disease and mild cognitive impairment: a cross-sectional study. *The Lancet. Neurology***11**, 679–687 (2012).
23. Nagano-Saito, A. *et al.* Effect of mild cognitive impairment on the patterns of neural activity in early parkinson's disease. *Neurobiology of Aging***35**, 223–231 (2014).
24. Hanakawa, T., Fukuyama, H., Katsumi, Y., Honda, M. & Shibasaki, H. Enhanced lateral premotor activity during paradoxical gait in parkinson's disease. *Annals of Neurology***45**, 329–336 (1999).
25. Wu, T. *et al.* Attention to automatic movements in Parkinson's disease: Modified automatic mode in the striatum. *Cerebral Cortex***25**, 3330–3342 (2015).
26. Nagano-Saito, A. *et al.* Patterns of longitudinal neural activity linked to different cognitive profiles in Parkinson's disease. *Frontiers in Aging Neuroscience***8**, 275 (2016).
27. Nagano-Saito, A. *et al.* Why Is Aging a Risk Factor for Cognitive Impairment in Parkinson's Disease?-A Resting State fMRI Study. *Frontiers in neurology***10**, 267 (2019).
28. Basser, P. J., Pajevic, S., Pierpaoli, C., Duda, J. & Aldroubi, A. In vivo fiber tractography using DT-MRI data. *Magnetic Resonance in Medicine***44**, 625–632 (2000).
29. Basser, P. J., Mattiello, J. & LeBihan, D. MR diffusion tensor spectroscopy and imaging. *Biophysical journal***66**, 259–267 (1994).
30. Conturo, T. E. *et al.* Tracking neuronal fiber pathways in the living human brain. *Proceedings of the National Academy of Sciences of the United States of America***96**, 10422–10427 (1999).
31. Mori, S., Crain, B. J., Chacko, V. P. & van Zijl, P. C. Three-dimensional tracking of axonal projections in the brain by magnetic resonance imaging. *Annals of neurology***45**, 265–269 (1999).
32. Tournier, J.-D., Calamante, F. & Connelly, A. Robust determination of the fibre orientation distribution in diffusion MRI: non-negativity constrained super-resolved spherical deconvolution. *NeuroImage***35**, 1459–1472 (2007).
33. Descoteaux, M. & Deriche, R. Segmentation of Q-Ball images using statistical surface evolution. *Medical image computing and computer-assisted intervention : MICCAI ... International Conference on Medical Image Computing and Computer-Assisted Intervention***10**, 769–776 (2007).
34. Ozarslan, E., Shepherd, T. M., Vemuri, B. C., Blackband, S. J. & Mareci, T. H. Resolution of complex tissue microarchitecture using the diffusion orientation transform (DOT). *NeuroImage***31**, 1086–1103

(2006).

35. Tuch, D. S. Q-ball imaging. *Magnetic resonance in medicine***52**, 1358–1372 (2004).
36. Jensen, J. H., Helpern, J. A., Ramani, A., Lu, H. & Kaczynski, K. Diffusional kurtosis imaging: the quantification of non-gaussian water diffusion by means of magnetic resonance imaging. *Magnetic resonance in medicine***53**, 1432–1440 (2005).
37. Atkinson-Clement, C., Pinto, S., Eusebio, A. & Coulon, O. Diffusion tensor imaging in Parkinson's disease: Review and meta-analysis. *NeuroImage: Clinical* vol. 16 98–110 (2017).
38. Wen, M.-C. *et al.* White matter microstructural characteristics in newly diagnosed Parkinson's disease: An unbiased whole-brain study. *Scientific Reports***6**, 35601 (2016).
39. Taylor, K. I., Sambataro, F., Boess, F., Bertolino, A. & Dukart, J. Progressive Decline in Gray and White Matter Integrity in de novo Parkinson's Disease: An Analysis of Longitudinal Parkinson Progression Markers Initiative Diffusion Tensor Imaging Data. *Frontiers in Aging Neuroscience***10**, 318 (2018).
40. Georgiopoulos, C. *et al.* Olfactory Impairment in Parkinson's Disease Studied with Diffusion Tensor and Magnetization Transfer Imaging. *Journal of Parkinson's Disease***7**, 301–311 (2017).
41. Kamagata, K. *et al.* Relationship between cognitive impairment and white-matter alteration in Parkinson's disease with dementia: tract-based spatial statistics and tract-specific analysis. *European radiology***23**, 1946–1955 (2013).
42. Deng, B. *et al.* Diffusion tensor imaging reveals white matter changes associated with cognitive status in patients with Parkinson's disease. *American journal of Alzheimer's disease and other dementias***28**, 154–164 (2013).
43. Matsui, H. *et al.* Wisconsin Card Sorting Test in Parkinson's disease: diffusion tensor imaging. *Acta neurologica Scandinavica***116**, 108–112 (2007).
44. Zheng, Z. *et al.* DTI correlates of distinct cognitive impairments in Parkinson's disease. *Human brain mapping***35**, 1325–1333 (2014).
45. Wiegell, M. R., Larsson, H. B. & Wedeen, V. J. Fiber crossing in human brain depicted with diffusion tensor MR imaging. *Radiology***217**, 897–903 (2000).
46. Kamagata, K. *et al.* Diffusional kurtosis imaging of cingulate fibers in Parkinson disease: Comparison with conventional diffusion tensor imaging. *Magnetic Resonance Imaging***31**, 1501–1506 (2013).
47. Raffelt, D. *et al.* Apparent Fibre Density: a novel measure for the analysis of diffusion-weighted magnetic resonance images. *NeuroImage***59**, 3976–3994 (2012).
48. Dell'Acqua, F. & Catani, M. Structural human brain networks: hot topics in diffusion tractography. *Current opinion in neurology***25**, 375–383 (2012).
49. Tournier, J.-D. *et al.* MRtrix3: A fast, flexible and open software framework for medical image processing and visualisation. *NeuroImage***202**, 116137 (2019).
50. Pfefferbaum, A. *et al.* Age-related decline in brain white matter anisotropy measured with spatially corrected echo-planar diffusion tensor imaging. *Magnetic resonance in medicine***44**, 259–268

(2000).

51. Ennis, D. B. & Kindlmann, G. Orthogonal tensor invariants and the analysis of diffusion tensor magnetic resonance images. *Magnetic resonance in medicine***55**, 136–146 (2006).
52. Peterson, D. J. *et al.* Increased regional fractional anisotropy in highly screened attention-deficit hyperactivity disorder (ADHD). *Journal of child neurology***26**, 1296–1302 (2011).
53. Arkadir, D., Bergman, H. & Fahn, S. Redundant dopaminergic activity may enable compensatory axonal sprouting in Parkinson disease. *Neurology***82**, 1093–1098 (2014).
54. Delaveau, P. *et al.* Dopaminergic modulation of the default mode network in Parkinson's disease. *European Neuropsychopharmacology***20**, 784–792 (2010).
55. Krajcovicova, L., Mikl, M., Marecek, R. & Rektorova, I. The default mode network integrity in patients with Parkinson's disease is levodopa equivalent dose-dependent. *Journal of Neural Transmission***119**, 443–454 (2012).
56. Van Eimeren, T., Monchi, O., Ballanger, B. & Strafella, A. P. Dysfunction of the default mode network in Parkinson disease: A functional magnetic resonance imaging study. *Archives of Neurology***66**, 877–883 (2009).
57. Watson, R. *et al.* Characterizing dementia with Lewy bodies by means of diffusion tensor imaging. *Neurology***79**, 906–914 (2012).
58. Suillivan, E. V & Pfefferbaum, A. Neuroradiological characterization of normal adult ageing. *The British Journal of Radiology***80**, S99–S108 (2007).
59. Bzdok, D. *et al.* Subspecialization in the human posterior medial cortex. *NeuroImage***106**, 55–71 (2015).
60. Beaulieu, C. The basis of anisotropic water diffusion in the nervous system - A technical review. *NMR in Biomedicine* vol. 15 435–455 (2002).
61. Braak, H., Rüb, U. & Del Tredici, K. Cognitive decline correlates with neuropathological stage in Parkinson's disease. *Journal of the Neurological Sciences***248**, 255–258 (2006).
62. Cavanna, A. E. & Trimble, M. R. The precuneus: A review of its functional anatomy and behavioural correlates. *Brain***129**, 564–583 (2006).
63. Scheck, S. M. *et al.* Structural connectivity of the anterior cingulate in children with unilateral cerebral palsy due to white matter lesions. *NeuroImage. Clinical***9**, 498–505 (2015).
64. Küpper, H. *et al.* Predicting hand function after hemidisconnection. *Brain : a journal of neurology***139**, 2456–2468 (2016).
65. Nagano-Saito, A. *et al.* Posterior dopamine D2/3 receptors and brain network functional connectivity. *Synapse***71**, (2017).
66. Inano, S., Takao, H., Hayashi, N., Abe, O. & Ohtomo, K. Effects of age and gender on white matter integrity. *AJNR. American journal of neuroradiology***32**, 2103–2109 (2011).
67. Michielse, S. *et al.* Selective effects of aging on brain white matter microstructure: a diffusion tensor imaging tractography study. *NeuroImage***52**, 1190–1201 (2010).

68. Hughes, A. J., Ben-Shlomo, Y., Daniel, S. E. & Lees, A. J. What features improve the accuracy of clinical diagnosis in parkinson's disease: A clinicopathologic study. *Neurology***42**, 1142–1146 (1992).
69. Hanganu, A. *et al.* White matter degeneration profile in the cognitive cortico-subcortical tracts in Parkinson's disease. *Movement disorders : official journal of the Movement Disorder Society***33**, 1139–1150 (2018).
70. Litvan, I. *et al.* Diagnostic criteria for mild cognitive impairment in Parkinson's disease: Movement Disorder Society Task Force guidelines. *Movement Disorders***27**, 349–356 (2012).
71. Nasreddine, Z. S. *et al.* The Montreal Cognitive Assessment, MoCA: a brief screening tool for mild cognitive impairment. *Journal of the American Geriatrics Society***53**, 695–699 (2005).
72. Salat, D. H. *et al.* Regional white matter volume differences in nondemented aging and Alzheimer's disease. *NeuroImage***44**, 1247–1258 (2009).
73. Desikan, R. S. *et al.* An automated labeling system for subdividing the human cerebral cortex on MRI scans into gyral based regions of interest. *NeuroImage***31**, 968–980 (2006).
74. Wassermann, D. *et al.* The white matter query language: a novel approach for describing human white matter anatomy. *Brain Structure and Function***221**, 4705–4721 (2016).
75. Nagano-Saito, A. *et al.* Effect of mild cognitive impairment on the patterns of neural activity in early Parkinson's disease. *Neurobiology of aging***35**, 223–231 (2014).
76. Wu, Y., Sun, D., Wang, Y., Wang, Y. & Ou, S. Segmentation of the Cingulum Bundle in the Human Brain: A New Perspective Based on DSI Tractography and Fiber Dissection Study. *Frontiers in Neuroanatomy***10**, 84 (2016).
77. Burgess, P. & Shallice, T. *The hayling and brixton tests. Test manual.* (Thames Valley Test Company, 1997).
78. Schmidt, M. *Rey auditory verbal learning test: A handbook.* (Western Psychological Services, 1996).

Tables

Table 1. Correlation analysis of FA and AFD index in HV and PD.

		FA				AFD					
		Precuneus	Isthmus	Posterior cingulate	Angerior cingulate	PCG-PCN	PCG-PHG	PCN-PHG	PCN-Cortex	PCN-Local	PCN-Cross
HV											
Brixton	r	-0.299	-0.096	0.144	0.028	***-0.449***	-0.025	0.386	0.140	0.093	-0.015
	p	0.261	0.723	0.594	0.918	***0.081***	0.926	0.139	0.604	0.733	0.956
RAVLT	r	**0.691**	-0.168	-0.013	0.065	***0.432***	0.351	-0.152	-0.025	-0.104	0.299
	p	**0.003**	0.534	0.963	0.812	***0.094***	0.183	0.573	0.928	0.702	0.260
Age	r	***0.440***	-0.069	-0.273	0.045	**0.511**	-0.017	-0.210	-0.197	0.100	0.230
	p	***0.088***	0.801	0.307	0.868	**0.043**	0.951	0.436	0.465	0.713	0.392
PD											
Brixton	r	**0.350**	-0.044	0.168	0.149	-0.031	0.119	0.023	0.045	0.047	0.096
	p	**0.031**	0.792	0.312	0.371	0.852	0.476	0.893	0.789	0.777	0.567
RAVLT	r	-0.093	-0.016	0.082	0.197	**-0.382**	0.144	-0.096	-0.083	0.062	0.134
	p	0.577	0.926	0.625	0.237	**0.018**	0.389	0.567	0.621	0.713	0.424
Age	r	**-0.390**	**-0.448**	**-0.409**	**-0.571**	-0.173	-0.252	-0.052	0.248	-0.078	**-0.610**
	p	**0.015**	**0.005**	**0.011**	**< 0.001**	0.298	0.127	0.759	0.133	0.642	**< 0.001**

PCG; Posterior cingulate gyrus, PCN; Precuneus, PHV; Parahippocampal gyrus. Bold letters indicate significant correlation (P < 0.05), and bold italic letters indicate marginally significant correlation (p < 0.1).

Figures

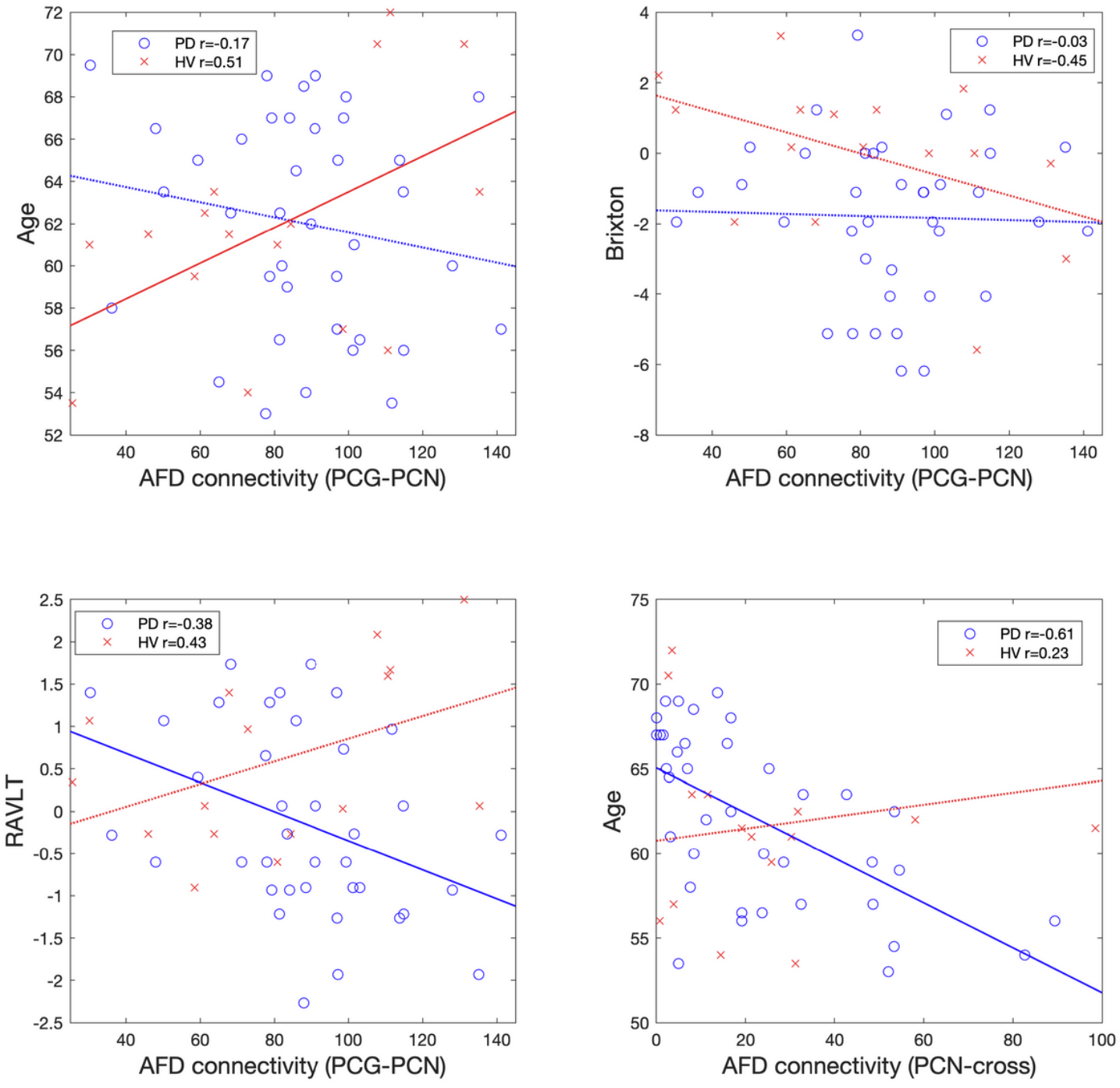

Figure 5

Correlation of AFD connectivity with age, and cognitive Z scores.